Prompt and delayed dissociation of N_2O^{2+} induced by highly-charged-ion collisions

Xi Zhao,[1] Xu Shan,[1,*] Xiaolong Zhu,[2] Lei Chen,[1] Zhenjie Shen,[1] Wentian Feng,[2] Dalong Guo,[2] Dongmei Zhao,[2] Ruitian Zhang,[2] Yong Gao,[2] Zhongkui Huang,[2] Shaofeng Zhang,[2] Xinwen Ma,[2,†] and Xiangjun Chen[1]

[1]*Hefei National Laboratory for Physical Sciences at the Microscale and Department of Modern Physics, University of Science and Technology of China, Hefei, 230026, China*

[2]*Institute of Modern Physics, Chinese Academy of Sciences, Lanzhou, 730000, China*

(Received 10 September 2020; accepted 17 December 2020; published 4 January 2021)

The prompt and delayed dissociations of $N_2O^{2+} \rightarrow N^+ + NO^+$ induced by electron capture collisions of 56-keV/u Ne^{4+} and Ne^{8+} ions are studied by measuring ion-pair fragments and charge-changed projectiles in triple coincidence. For the prompt dissociation, the kinetic energy release (KER) distributions are obtained and indicate this process is mainly attributed to the decay of the low-lying $1\ ^3\Sigma^-$ state N_2O^{2+} into $N^+(^3P) + NO^+(^1\Sigma^+)$. For the delayed dissociation, since it is of difficulty to directly retrieve three-dimensional momentum vectors of ionic fragments for all the events from N_2O^{2+} dissociation in flight, an alternative way is proposed to only catch and analyze the events from which the N_2O^{2+} breakup direction is perpendicular to the time-of-flight axis. The KER distributions for these events are obtained and the metastable states of N_2O^{2+} are confirmed to be $1\ ^3\Pi$ and $2\ ^3\Pi$. The survival time spectra for the metastable N_2O^{2+} are also extracted and the mean lifetimes for the $1\ ^3\Pi$ and $2\ ^3\Pi$ conjoin, as well as the lifetimes for the identified individual metastable state, are deduced both in Ne^{8+} and Ne^{4+} collision experiments.

DOI: 10.1103/PhysRevA.103.012802

I. INTRODUCTION

As one or more electrons are stripped from a molecule in collision with energetic ions, electrons, or photons, the molecular ion is formed and ready to break up due to the Coulomb repulsion. The dissociation process often takes place on fast timescales (typically subpicosecond) [1–3]. Not all dissociation processes, however, proceed so quickly. Molecular ion also can exist in metastable states that lead to dissociation happening on long timescales from picoseconds to even seconds [4–8]. Such two kinds of fragmentation processes, called prompt and delayed dissociations, are dependent on the relevant electronic states of the molecular ion and the mechanisms responsible for decay. Various spectroscopy techniques and multiparticle coincidence methods associated with electrons, ions, and photons [4,5], especially the recoil momentum spectroscopy or reaction microscope [9,10], allow us to explore the fragmentation dynamics for both prompt and delayed dissociations of molecular ions, as well as to determine the lifetime of metastable molecular ions. Besides the tremendous progress on the prompt dissociation of molecular ions [11–17], investigation on the formation and decay of metastable molecular ions experimentally and theoretically has been a prominent field of research [4–8,18–27].

Nitrous oxide (N_2O) is one of the prototype molecules whose dication may exist in both repulsive and metastable states that undergo the prompt and delayed dissociations. The fragmentation of N_2O^{2+} has been extensively studied experimentally and theoretically [8,22–39]. Two distinct charge separation channels for the prompt dissociations were observed, i.e., $N_2O^{2+} \rightarrow N^+ + NO^+$ and $N_2O^{2+} \rightarrow N_2^+ + O^+$. The delayed dissociation arising from the metastable N_2O^{2+} only occurred for the N-N bond breakup. The lifetime of metastable N_2O^{2+} has been an object of many experimental and theoretical efforts. For example, Newton and Sciamanna measured the lifetime of metastable N_2O^{2+} to be 660 ± 70 ns for the first time by studying the intensity of the metastable peak in mass spectra as a function of the ion accelerating potential [23]. Field and Eland [8] introduced a method to extract the lifetime of metastable dication decaying in flight by fitting the simulated time-of-flight (TOF) difference spectrum to the measured one and deduced a mean lifetime of 450^{+250}_{-200} ns for N_2O^{2+}. In subsequent studies, Alagia *et al.* [24] estimated the lifetime no longer than $\sim 10^{-6}$ s, while Kübel *et al.* [26] estimated the lifetime to be a few hundred nanoseconds. Khan *et al.* [27], using a similar technique of Field and Eland [8], inferred a mean lifetime of 660 ± 30 ns in a 5-keV electron collision experiment. Taylor *et al.* [25] revealed one conclusive and another probable metastable state of the N_2O^{2+} dication and assigned respectively as $1\ ^3\Pi$ at 38.5 eV and $2\ ^3\Pi$ at 42.5 eV by comprising photoionization and fluorescent experiments with theoretical calculations on the electronic states of N_2O^{2+}. They also theoretically predicted that $1\ ^3\Pi$ N_2O^{2+} decays via a fluorescent transition to the ground-state $1\ ^3\Sigma^-$ which dissociates quickly into $N^+ + NO^+$, and an identical mechanism may also occur for $2\ ^3\Pi$ N_2O^{2+}. Actually, an alternative decay mechanism for metastable molecular ions such as the tunneling dissociation may also take place. To identify the decay mechanism of

*xshan@ustc.edu.cn
†x.ma@impcas.ac.cn

metastable N_2O^{2+} and determine its lifetime for the specific dissociation route are shown to pose fascinating questions. But the relevant research reports are very scarce.

In the present work, we focus on the prompt and delayed dissociations of $N_2O^{2+} \rightarrow N^+ + NO^+$ induced by 56-keV/u Ne^{4+} and Ne^{8+} collisions. For the prompt dissociation, the three-dimensional momenta of ionic fragments measured in coincidence are used to reconstruct the kinetic energy release (KER) spectra which revealed this process mainly comes from the fast decay of $1\,^3\Sigma^-$ state of N_2O^{2+} into $N^+(^3P) + NO^+(^1\Sigma^+)$ with the help of the calculations of Taylor *et al.* [25]. For the delayed dissociation, because of N_2O^{2+} decaying in flight, it is impossible to directly retrieve the three-dimensional momenta of ionic fragments for all the events. A method is introduced to only catch and analyze the events in which the initial direction of ionic fragments from N_2O^{2+} dissociating in flight is perpendicular to the TOF axis. The corresponding KER distribution is obtained and the metastable states of N_2O^{2+} are identified to be $1\,^3\Pi$ and $2\,^3\Pi$ according to the calculation of Taylor *et al.* [25]. The survival time spectra for the metastable state-selected N_2O^{2+} are also extracted and the corresponding lifetimes are deduced for the tunneling dissociation route in both Ne^{4+} and Ne^{8+} experiments, respectively.

II. EXPERIMENTAL METHOD

The present experiments are carried out by the collision of charged ions with gas-phase N_2O molecules using the reaction microscope on the 320-kV platform for multidisciplinary research with highly charged ions at the Institute of Modern Physics in Lanzhou. The details of the experimental setup have been presented previously [40,41]. The projectile ions are produced in the electron cyclotron resonance ion source and accelerated to the experimental energy for collisions. In this work, two independent experiments have been done, and the 56-keV/u Ne^{8+} and Ne^{4+} projectiles are employed in the experiments. After being collimated by two sets of adjustable slits and purified by several sets of electrostatic deflectors, the ion beam was transported to the target chamber and intersected with a cold supersonic N_2O gas jet which is introduced into the reaction chamber through a nozzle of 0.03-mm diameter and picked up by two skimmers of 0.05-mm diameter. A Wiley-McLaren type TOF system [42], having a 107.5-mm-length acceleration region and a 215-mm-length field-free drifting distance with a length ratio of 1:2, is employed to extract and transfer the ionic products of the target into a time- and position-sensitive detector (PSD-R). The primary beam of projectiles is collected by a Faraday cup, and the charge-changed projectile ions are analyzed by a pair of electrostatic deflectors downstream of the collision zone combined with another position-sensitive detector (PSD-P). All position-sensitive detectors are built as a combination of the microchannel plate with the standard delay line anode. The signal and data acquisition system was triggered by the signal from the PSD-P, and the recoil ions were recorded in coincidence with the scattered projectile ions. The information on the position and TOF of ionic fragments is recorded event by event. In the offline data analysis, the three-dimensional momentum vectors of each ion detected can be obtained by the observed TOF and position (x, y). Through the correlation analysis on the TOF and momentum conservation of ion-pair fragments, as well as the charge states of the scattered projectile, the reaction channels for the two-body Coulomb explosion induced by transfer ionization (TI) and double-electron capture (DC) processes can be determined.

TABLE I. The branching ratios for the prompt and delayed dissociations of $N_2O^{2+} \rightarrow N^+ + NO^+$.

	56 keV/u Ne^{4+}		56 keV/u Ne^{8+}	
	Ne^{3+}	Ne^{2+}	Ne^{7+}	Ne^{6+}
Prompt	96.51%	0.51%	95.09%	1.24%
Delayed	2.98%		3.62%	0.05%
Ratio	32/1		24/1	25/1

III. RESULTS AND DISCUSSION

A. Ion-ion TOF coincidence spectra

Various fragmentation channels are produced by the impact of N_2O molecules with Ne^{4+} and Ne^{8+} projectiles. Here we only concentrate on the two-body breakup of N_2O^{2+}. Two kinds of ion-pair channels of $N_2O^{2+} \rightarrow N^+ + NO^+$ and $N_2^+ + O^+$ can be observed in the TI and DC collisions of Ne^{4+} and Ne^{8+} projectiles, as the ion-ion TOF coincidence spectra showed in Fig. 1. Due to the conservation of momentum, the TOF correlation islands in the ion-ion coincidence spectra for the events of the two-body breakup of N_2O^{2+} display the sharp diagonal lines. The observed prominent diagonal lines are corresponding to the prompt dissociation of N_2O^{2+}. A long tail extending from the $NO^+ + N^+$ coincidence trace is also observed and ascribed to the metastable N_2O^{2+} dissociating in flight along the axis of the TOF system, named as the delayed dissociation. Such long tails have been observed previously [8,23–39]. The trace for N_2O^{2+} decay in flight can be divided into two parts, the "tail" and "V" patterns. The tail indicates that the delayed dissociation takes place in the acceleration zone of the TOF system while the V in the field-free drifting zone [25]. The simulation for the trace of N_2O^{2+} dissociating in flight is performed by varying the delayed times of N_2O^{2+} breakup and simulating the TOFs of two fragment ions under the experimental condition, as the solid square symbols displayed in Fig. 1(c), agreeing with the measurement well.

The true events for prompt and delayed dissociation channels of N_2O^{2+} can be obtained by further analyzing the correlation of ion-pair momenta and eliminating the false events in TOF coincidence spectra. Obviously, the TI induced dissociative reactions are dominant, as shown in Fig. 1. For two prompt dissociation channels of N_2O^{2+}, the ratio of $NO^+ + N^+$ and $N_2^+ + O^+$ is about 64:36, very close to the previous data from the ion collision [36,37], but smaller than those from photon and electron experiments (80:20 or 75:25) [24,28,32,36], as well as the theoretical prediction (75:25) [33]. It is worthwhile to note that the branching ratios for the prompt and delayed dissociations of $N_2O^{2+} \rightarrow N^+ + NO^+$ are also obtained as listed in Table I. One can see that the TI reactions dominate in both Ne^{4+} and Ne^{8+} collision

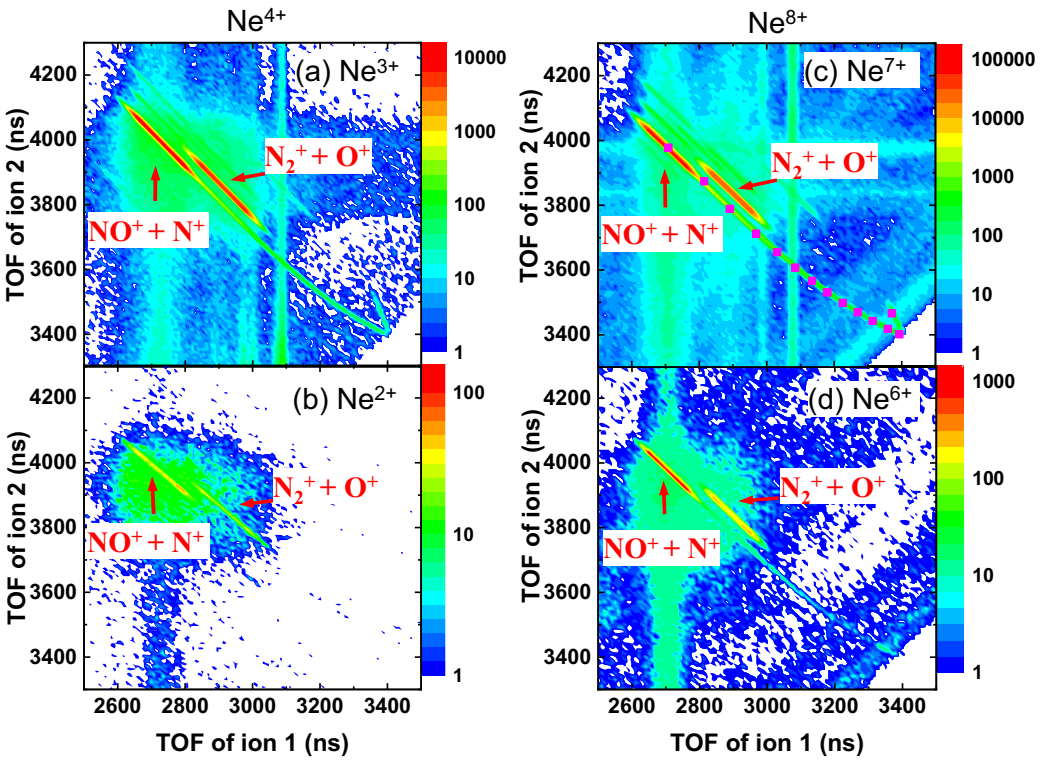

FIG. 1. The ion-ion TOF coincidence spectra of the fragments of N_2O^{2+} between the first hit ion and the second one. (a) for the TI of Ne^{4+}. (b) for the DC of Ne^{4+}. (c) for the TI of Ne^{8+}. (d) for the DC of Ne^{8+}. The square solid dots in (c) represent the simulated results.

experiments. The DC channel enhances obviously with the increase of the projectile charges, and the same case also appears for the ratios of the delayed dissociations relative to the prompt ones. One has to bear in mind that, for highly charged ions at this low impact energy, double electrons captured from loosely bound target should be mainly populated on the doubly excited states of the projectile, which will predominately decay via Auger or autoionizing process for light ions. Thus, the TI channel essentially originates from the DC process. For Ne^{8+} projectile, it has more low-lying empty orbitals and stronger Coulomb potential than Ne^{4+}, which may result in larger DC cross sections. Note that the delayed dissociation in the DC channel of Ne^{4+} is not observed, as depicted in Fig. 1(b), due to very poor statistics counts.

B. Prompt dissociation channels of N_2O^{2+}

As mentioned above, two kinds of prompt dissociation channels have been identified from the TOF correlation spectra in Fig. 1, namely, deoxygenation ($N_2O^{2+} \rightarrow O^+ + N_2{}^+$) and denitrogenation ($N_2O^{2+} \rightarrow N^+ + NO^+$). The KER distributions for these two prompt channels are deduced and shown in Figs. 2 and 3, respectively. One can see that the KER spectra of $N_2O^{2+} \rightarrow O^+ + N_2{}^+$ induced by the TI and DC processes of Ne^{4+} and Ne^{8+} projectiles show the similar structures, the same case for $N_2O^{2+} \rightarrow N^+ + NO^+$, suggesting that the KER features are not sensitive to the reaction processes which induced almost identical states of N_2O^{2+} prior to dissociation. This confirms the above-mentioned statement that the TI originates from the DC process, namely, $Ne^{q+} + N_2O \rightarrow [Ne^{(q-2)+}]^{**} + [N_2O^{2+}]^{**}$, followed closely by a projectile stabilization with autoionizing cascades $[Ne^{(q-2)+}]^{**} \rightarrow Ne^{(q-1)+} + e^-$. Such a phenomenon is similar to the observation of Chen *et al.* using 5.7-keV/u Xe^{15+} projectile [37].

As shown in Fig. 2, the KER spectra for $N_2O^{2+} \rightarrow O^+ + N_2{}^+$ show a noticeable peak at about 5.8 eV, a shoulder around 7.0 eV, and a high-energy tail starting from 9.5 eV. The present observations on the first two KER structures are in good accordance with the previous measurements [26,27,37,38]. According to the measured KER together with the potential-energy curves (PECs) of N_2O^{2+} calculated by Taylor *et al.* [25], the presently observed peak at ~5.8 eV can be ascribed to the decay of $N_2O^{2+}(X\,^3\Sigma^-) \rightarrow O^+(^4S) + N_2{}^+(^2\Sigma_g^+)$, and the shoulder should be attributed to the $N_2O^{2+}(1\,^3\Pi)$ dissociating into $O^+(^4S) + N_2{}^+(^2\Pi_u)$.

As for the prompt dissociation of $N_2O^{2+} \rightarrow N^+ + NO^+$, the KER spectra in Fig. 3 present a major peak at 6.8 eV and a broad shoulder around 9.0 eV. According to the calculations of Taylor *et al.* [25], the pronounced KER peak at 6.8 eV indicates that the N_2O^{2+} prefers the decay pathway of $N_2O^{2+}(1\,^3\Sigma^-) \rightarrow N^+(^3P) + NO^+(^1\Sigma^+)$, and an alternative route of N_2O^{2+} $(1\,^3\Pi)$ is fluorescent transitioning to the $1\,^3\Sigma^-$ state and then dissociating into $N^+(^3P) + NO^+(^1\Sigma^+)$. The broad shoulder at ~9.0 eV mainly indicates the dissociation $N_2O^{2+}(1\,^1\Pi, 1\,^1\Sigma^-) \rightarrow N^+(^1D) + NO^+(^1\Sigma^+)$ in view of the possible curve crossing of $1\,^1\Pi$ and $1\,^1\Sigma^-$ states.

C. Delayed dissociation for $N_2O^{2+} \rightarrow N^+ + NO^+$

As shown in Fig. 1, the delayed dissociation can be observed for the denitrogenation channels. In order to reveal its origin, the accurate KER spectra, together with the PECs

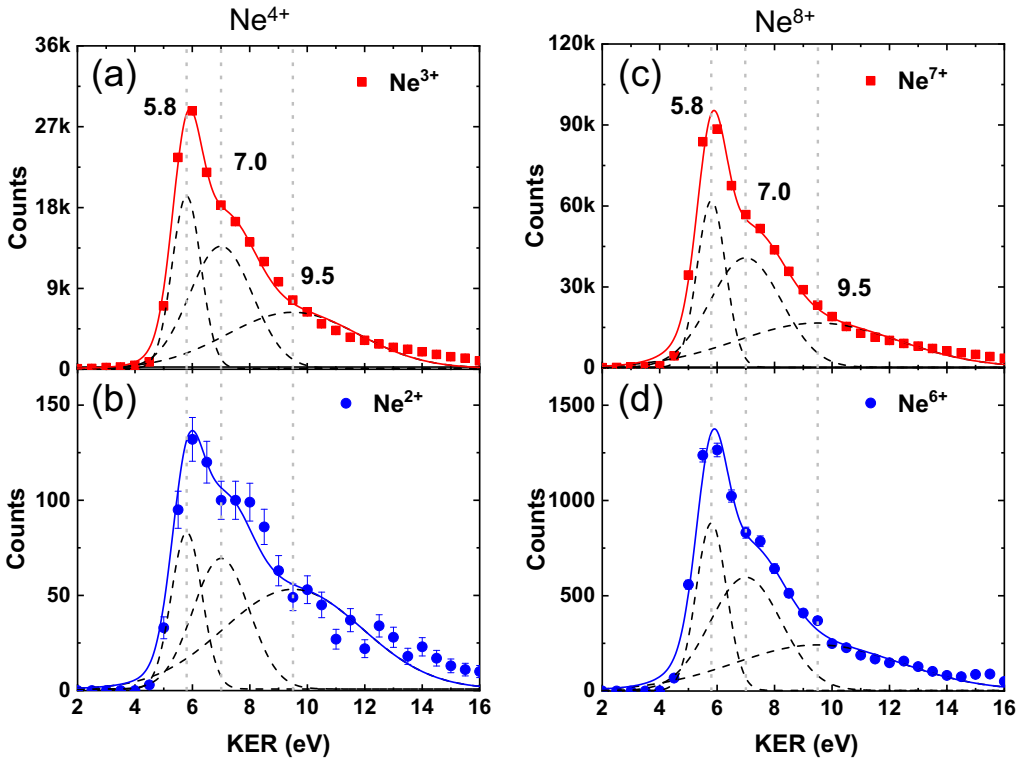

FIG. 2. The KER spectra for the prompt dissociation channel $N_2O^{2+} \rightarrow O^+ + N_2{}^+$. (a) for the TI of Ne^{4+}. (b) for the DC of Ne^{4+}. (c) for the TI of Ne^{8+}. (d) for the DC of Ne^{8+}. Gaussian peaks (dashed lines) are used to fit the experimental data (circular and square solid dots) and the solid lines represent the sum of their fitting.

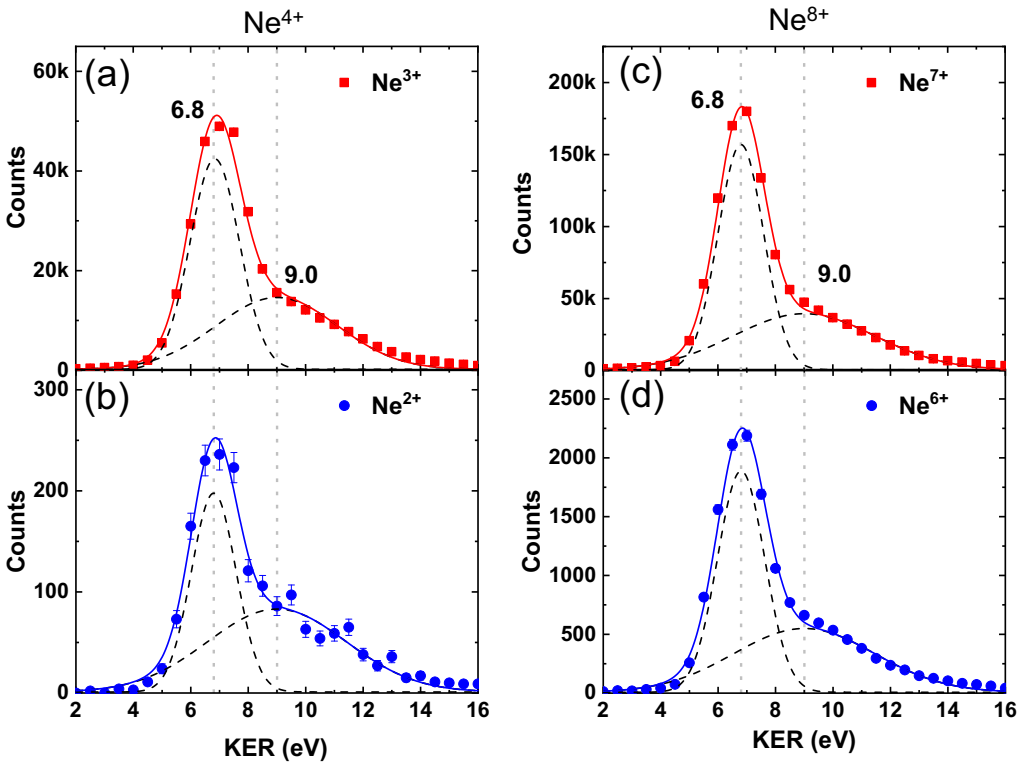

FIG. 3. The KER spectra for the prompt dissociation channel $N_2O^{2+} \rightarrow N^+ + NO^+$. (a) for the TI of Ne^{4+}. (b) for the DC of Ne^{4+}. (c) for the TI of Ne^{8+}. (d) for the DC of Ne^{8+}. Gaussian peaks (dashed lines) are used to fit the experimental data (circular and square solid dots) and the solid lines represent the sum of their fitting.

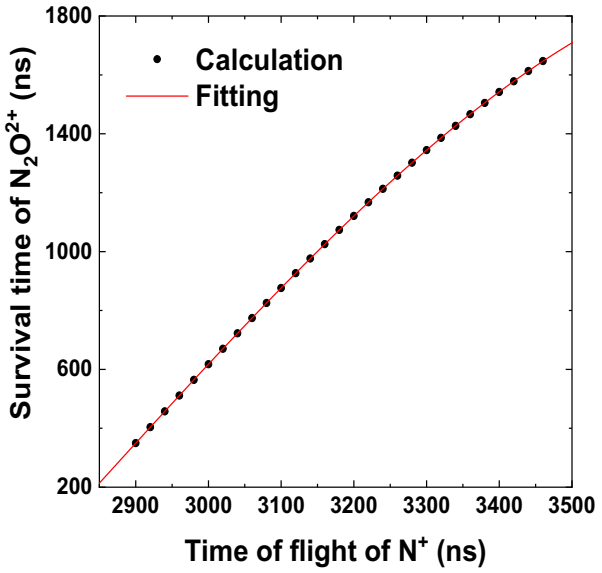

FIG. 4. The relationship of the survival time of N_2O^{2+} and the TOF of N^+ ions by numerically solving Newton's equations.

of N_2O^{2+}, are demanded. Usually the KER can be obtained by reconstructing the momentum vectors of ionic fragments from the direct and/or prompt dissociation events. But for the delayed dissociation, it is very hard to directly reconstruct the momentum vectors of ionic fragments from all the events. The reason is that the recorded flight times of fragments are not the actual TOF starting from the instant of breakup as the metastable N_2O^{2+} dissociating in flight along the axis of the TOF spectrometer. In this work, we overcome this difficulty by choosing the events that the initially ejected direction of ion-pair fragments is perpendicular to the TOF axis based on the facts, (i) the velocity of ionic fragments along the TOF axis is equal to that of N_2O^{2+} at the moment of dissociation. (ii) The distance between the positions of the ion-pair fragments with specific energy hitting on the ion detector is the farthest (maximum, noted as $d_{\max}$).

For the metastable molecular ions dissociating in flight whose fragments initially ejected perpendicular to the TOF axis, the real TOF of fragments and the survival time of N_2O^{2+} can be obtained via solving Newton's equations [Eqs. (1)–(3)] for the motion of parent ion N_2O^{2+} and daughter fragments in the given dc field and flight length for the TOF system.

$$\tfrac{1}{2}a_M t_M^2 + (a_M t_M)t_{ia} + \tfrac{1}{2}a_i t_{ia}^2 = \tfrac{1}{3}L, \tag{1}$$

$$(a_M t_M + a_i t_{ia})t_{if} = \tfrac{2}{3}L, \tag{2}$$

$$t_M + t_{ia} + t_{if} = T. \tag{3}$$

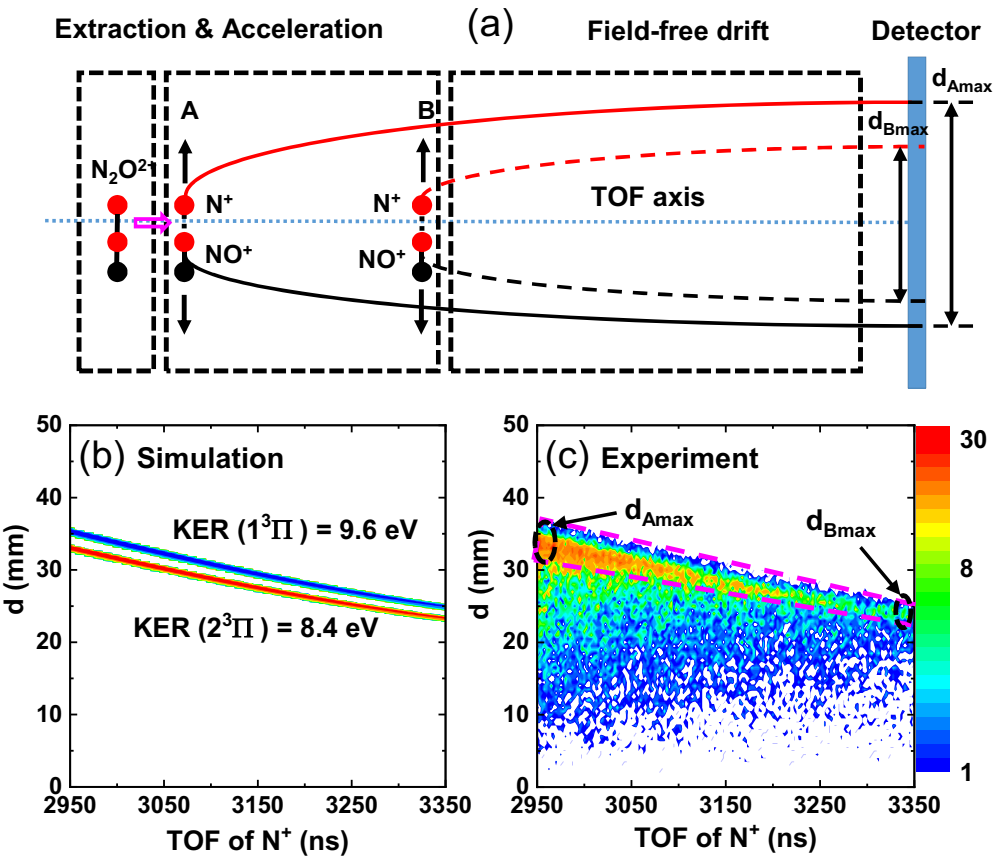

FIG. 5. (a) Schematic diagram for the TOF system and the trajectory of ionic fragments from the metastable N_2O^{2+} dissociation perpendicular to the TOF axis. (b) The simulated relationship between the maximum distance $d_{\max}$ and the TOF of N^+ fragment for N_2O^{2+} dissociation in flight perpendicular to the TOF axis. (c) The relationship between the distance of ion-pair fragments hit on the detector and the TOF of N^+ for all measured events from the delayed dissociation of $N_2O^{2+} \rightarrow N^+ + NO^+$ induced by the TI collision of Ne^{8+}. The region labeled by the dashed line represents the events for N^+ initially ejected perpendicular to the TOF axis.

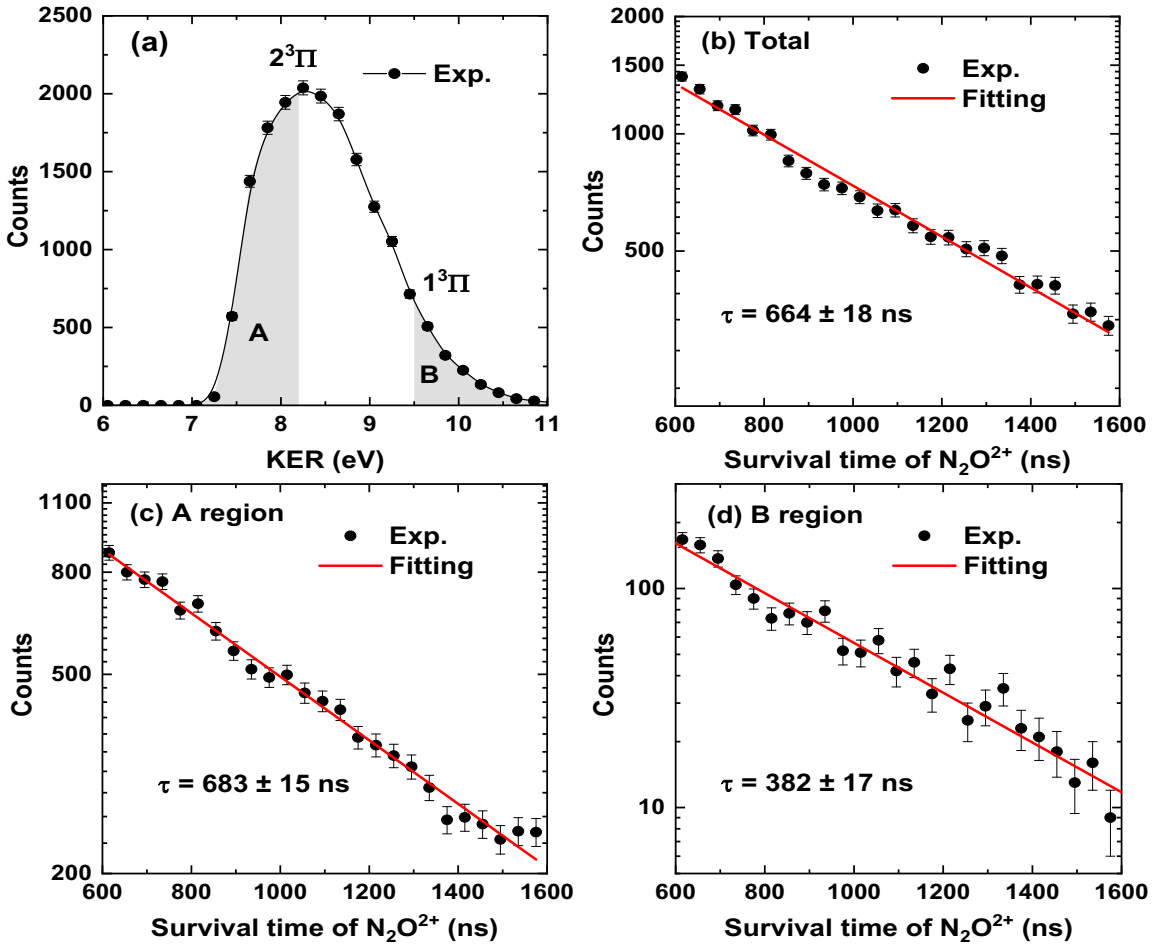

FIG. 6. The KER and lifetime spectra for the delayed dissociation of $N_2O^{2+} \rightarrow N^+ + NO^+$ induced by the TI collision of Ne^{8+}. (a) KER distribution. (b) Survival time spectrum for selecting total KER data. (c) Survival time spectrum for A region in (a). (d) Survival time spectrum for B region in (a).

Here, Eq. (1) represents the motion of parent and daughter ions in the acceleration region with the dc field while Eq. (2) indicates their motion in the field-free flight tube. a_M and t_M are the acceleration and survival time of N_2O^{2+}, respectively. a_{ia} and $t_{ia} (i = 1, 2)$ are the acceleration and the TOF in the acceleration region of N^+ or NO^+, respectively. L is the distance between the interaction point and the ion detector. t_{if} is the TOF of fragments drifting the field-free tube, and T is the total TOF of the ions.

Figure 4 shows the numerical solution of Eqs. (1)–(3) for the survival time of N_2O^{2+} relative to the TOF for N^+ ions under the present experimental conditions. Therefore, according to the measured TOF of N^+, it is easy to deduce the survival time of N_2O^{2+}, as well as the real TOF ($t = T - t_M$) of fragments from the instant of dissociation to reaching the detector. These enable us to reconstruct the accurate positions and momenta of ionic fragments, and then deduce the KER spectra for the delayed dissociation of the metastable N_2O^{2+}.

To realize the way proposed above, a vital step is to pick up the fragments initially ejected perpendicular to the TOF axis from all the recorded events. Figure 5(a) shows a schematic diagram for the TOF system and the trajectory of ionic fragments for N_2O^{2+} dissociation perpendicular to the TOF axis. The simulation is carried out for this delayed dissociation process of the metastable N_2O^{2+} to obtain the relationship between the maximum distance $d_{\max}$ and the total flying time T of N^+. In the simulation, the dc voltages applied are set to be the same as those in the present experiments. The initial angle of ionic fragments relative to the TOF axis is set to be $90° \pm 5°$ and the kinetic energies are referred to the KER values of 8.4 and 9.6 eV for the metastable $2\ ^3\Pi$ and $1\ ^3\Pi$ N_2O^{2+} tunneling dissociation into $N^+(^5S) + NO^+(^1\Sigma^+)$ and $N^+(^3P) + NO^+(^1\Sigma^+)$, respectively, according to the PEC calculations of Taylor *et al.* [25]. The simulated result is presented in Fig. 5(b). One can see that the maximum distance between the ion-pair fragments on the detector varies with the total TOF of N^+. Figure 5(c) shows the relationship between the distance of ion-pair fragments hit on the detector and the TOF of N^+ for all measured events from the delayed dissociation of $N_2O^{2+} \rightarrow N^+ + NO^+$ induced by the TI collision of Ne^{8+}. Obviously, the behavior of the data in the upper region as marked in the figure is in good accordance with the simulated result in Fig. 5(b), indicating that the data for the upper outmost region correspond to the metastable N_2O^{2+} dissociation perpendicular to the TOF axis. So we can select these data as marked in Fig. 5(c) and obtain the survival time of N_2O^{2+}

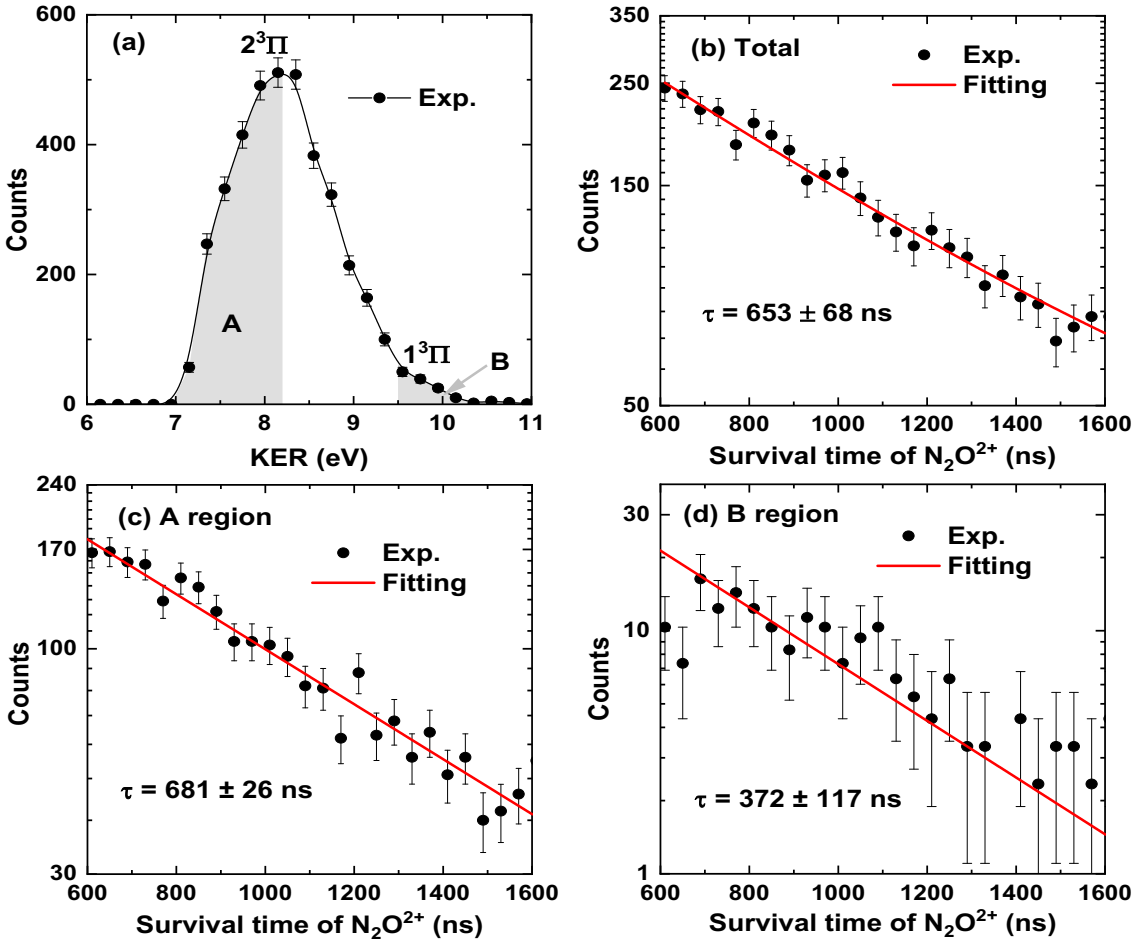

FIG. 7. The KER and lifetime spectra for the delayed dissociation of $N_2O^{2+} \rightarrow N^+ + NO^+$ induced by the TI collision of Ne^{4+}. (a) KER distribution. (b) Survival time spectrum for selecting total KER data. (c) Survival time spectrum for A region in (a). (d) Survival time spectrum for B region in (a).

with the aid of the relationship shown in Fig. 4. Then, the real TOF of N^+ from the produced moment to being detected and its position (x, y) on the detector are reconstructed, as well as the KER spectrum for the delayed dissociation of N_2O^{2+}.

Figure 6 presents the N_2O^{2+} survival time spectra and the KER distribution for the delayed dissociation of $N_2O^{2+} \rightarrow N^+ + NO^+$ induced by the TI collision of Ne^{8+}. In the same way, for the TI collision of Ne^{4+}, the lifetime spectra of N_2O^{2+} and the KER distribution for the delayed dissociation are also obtained and shown in Fig. 7. One can find that the KER spectra for the delayed dissociation of N_2O^{2+} in the Ne^{8+} and Ne^{4+} experiments display similar features, a major peak at about 8.2 eV and a weak structure around 9.5 eV. According to the previous PEC of N_2O^{2+} calculated by Taylor *et al.* [25], the major peak at ∼8.2 eV should be ascribed to the contribution of $N_2O^{2+}(2\ ^3\Pi)$ dissociating to $N^+(^5S) + NO^+(^1\Sigma^+)$ and the weak one at ∼9.4 eV should be attributed to the tunneling dissociation of $N_2O^{2+}(1\ ^3\Pi) \rightarrow N^+(^3P) + NO^+(^1\Sigma^+)$. Note that the fluorescent transition of N_2O^{2+} $(1\ ^3\Pi)$ to the ground state $1\ ^3\Sigma^-$ and subsequent dissociation may also possibly contribute to the major peak in view of the KER distribution for this decay route as shown in Fig. 3. In the previous works, Alagia *et al.* [24] and Taylor *et al.* [25] ascertained the $1\ ^3\Pi$ metastable state N_2O^{2+} in the double photoionization. Taylor *et al.* [25] also conjectured the possibility of $2\ ^3\Pi$ metastable state. The present experiments confirmed the formation of both $1\ ^3\Pi$ and $2\ ^3\Pi$ metastable state N_2O^{2+}.

For the lifetime of metastable N_2O^{2+}, as mentioned above, previous studies presented the mean lifetime of N_2O^{2+} in a few hundred nanoseconds [8,23–26]. In the present work, different from the previous methods, the lifetime of metastable N_2O^{2+} can be deduced from the survival time spectra for the KER-selected events, as shown in Figs. 6 and 7, respectively. It was well known that the survival time spectrum reveals the change of N_2O^{2+} population numbers decaying with the time, which can be described by an exponential equation $N = N_0 \exp(-\frac{t}{\tau})$, where N_0 is the total amount of the metastable N_2O^{2+} and τ is the lifetime. It allows us to determine the lifetime using the exponential function to fit the data of the survival time spectra. As illustrated in Figs. 6 and 7, the mean lifetime of the metastable N_2O^{2+} is obtained to be 664 ± 18 ns for the Ne^{8+} collision experiment, and 653 ± 68 ns for the Ne^{4+} experiment. The present results are in good accordance with the previous ones of 660 ± 70 ns [23] and 660 ± 30 ns [27]. Furthermore, in order to deduce the lifetime of individual metastable state, we figure out the KER-selected survival time spectra, corresponding to the $1\ ^3\Pi$ and $2\ ^3\Pi$, respectively.

The lifetime of the $1\ ^3\Pi$ metastable N_2O^{2+} through tunneling dissociation to $N^+(^3P) + NO^+(^1\Sigma^+)$ is obtained as 382 ± 17 ns for the Ne^{8+} experiment, and 372 ± 117 ns for the Ne^{4+} experiment. The lifetimes of the $2\ ^3\Pi$ metastable N_2O^{2+} are 683 ± 15 ns and 681 ± 26 ns, respectively. As for the longer lifetime for the $2\ ^3\Pi$ state than the $1\ ^3\Pi$, one probable factor, we think, is that the survival time spectra selected presently for the $2\ ^3\Pi$ state may be contaminated by the contribution of the $1\ ^3\Pi$ N_2O^{2+} fluorescent transition to the $1\ ^3\Sigma^-$ and then dissociating. Taylor *et al.* [25] theoretically predicted the fluorescent decay time of the $1\ ^3\Pi$ N_2O^{2+} is more than 600 ns but for a few tens of nanoseconds for the $2\ ^3\Pi$ state.

IV. CONCLUSION

The prompt and delayed dissociations of $N_2O^{2+} \rightarrow N^+ + NO^+$ have been studied by using the 56-keV/u Ne^{4+} and Ne^{8+} collision experiments. For the prompt dissociation, the measured KER spectra revealed this process mainly comes from the fast decay of $1\ ^3\Sigma^-$ state N_2O^{2+} into $N^+(^3P) + NO^+(^1\Sigma^+)$ with the help of the calculations of Taylor *et al.* [25]. For the delayed dissociation, a method was developed to retrieve the KER distribution and the survival time spectra of metastable N_2O^{2+}. The KER spectra for the delayed dissociation of N_2O^{2+} have been obtained, confirming that two metastable states of N_2O^{2+}, $1\ ^3\Pi$ and $2\ ^3\Pi$, are present. The survival time spectra for these two metastable N_2O^{2+} are also extracted and the mean lifetime of the metastable N_2O^{2+} is obtained to be 664 ± 18 ns in the Ne^{8+} experiment and 653 ± 68 ns in the Ne^{4+} experiment, agreeing with the previous results well. Furthermore, the lifetime of individual $1\ ^3\Pi$ state N_2O^{2+} via tunneling dissociation into $N^+(^3P) + NO^+(^1\Sigma^+)$ is retrieved to be 382 ± 17 ns in the Ne^{8+} experiment, and 372 ± 117 ns in the Ne^{4+} experiment, respectively. The present methods can be extended to retrieve the direct information for revealing the decay of the metastable molecular ions in the related research fields.

ACKNOWLEDGMENTS

This work is supported by the National Key Research and Development Program of China (Grant No. 2017YFA0402300), the Strategic Priority Research Program of Chinese Academy of Sciences (Grant No. XDB34000000), and the Science Challenge Project (Grant No. TZ2016005). X.M. was supported in part by the ExtreMe Matter Institute EMMI at the GSI Helmholtzzentrum fuer Schwerionenphysik, Darmstadt, Germany. The authors also thank the staff of the 320-kV platform for multidisciplinary research with highly charged ions at the Institute of Modern Physics, Chinese Academy of Sciences, for their technical support.

[1] T. Osipov, C. L. Cocke, M. H. Prior, A. Landers, T. Weber, O. Jagutzki, L. Schmidt, H. Schmidt-Böcking, and R. Dörner, Phys. Rev. Lett. **90**, 233002 (2003).

[2] T. Ergler, A. Rudenko, B. Feuerstein, K. Zrost, C. D. Schröter, R. Moshammer, and J. Ullrich, Phys. Rev. Lett. **97**, 193001 (2006).

[3] A. S. Chatterley, F. Lackner, D. M. Neumark, S. R. Leone, and O. Gessner, Phys. Chem. Chem. Phys. **18**, 14644 (2016).

[4] D. Mathur, Phys. Rep. **391**, 1 (2004).

[5] S. D. Price, Int. J. Mass Spectrom. Ion Phys. **260**, 1 (2007).

[6] D. Mathur, L. H. Andersen, P. Hvelplund, D. Kella, and C. P. Safvan, J. Phys. B **28**, 3415 (1995).

[7] L. H. Andersen, J. H. Posthumus, O. Vahtras, H. Ågren, N. Elander, A. Nunez, A. Scrinzi, M. Natiello, and M. Larsson, Phys. Rev. Lett. **71**, 1812 (1993).

[8] T. A. Field and J. H. D. Eland, Chem. Phys. Lett. **211**, 436 (1993).

[9] R. Dörner, V. Mergel, O. Jagutzki, L. Spielberger, J. Ullrich, R. Moshammer, and H. Schmidt-Böcking, Phys. Rep. **330**, 95 (2000).

[10] J. Ullrich, R. Moshammer, A. Dorn, R. Dörner, L. P. H. Schmidt, and H. Schmidt-Böcking, Rep. Prog. Phys. **66**, 1463 (2003).

[11] N. Neumann, D. Hant, L. P. H. Schmidt, J. Titze, T. Jahnke, A. Czasch, M. S. Schöffler, K. Kreidi, O. Jagutzki, H. Schmidt-Böcking, and R. Dörner, Phys. Rev. Lett. **104**, 103201 (2010).

[12] C. Wu, C. Wu, D. Song, H. Su, Y. Yang, Z. Wu, X. Liu, H. Liu, M. Li, Y. Deng, Y. Liu, L.-Y. Peng, H. Jiang, and Q. Gong, Phys. Rev. Lett. **110**, 103601 (2013).

[13] E. Wang, X. Shan, Z. Shen, M. Gong, Y. Tang, Y. Pan, K.-C. Lau, and X. Chen, Phys. Rev. A **91**, 052711 (2015).

[14] M. Pitzer, M. Kunitski, A. S. Johnson, T. Jahnke, H. Sann, F. Sturm, L. P. H. Schmidt, H. Schmidt-Böcking, R. Dörner, J. Stohner, J. Kiedrowski, M. Reggelin, S. Marquardt, A. Schießer, R. Berger, and M. S. Schöffler, Science **341**, 1096 (2013).

[15] X. Xie, S. Roither, M. Schöffler, E. Lötstedt, D. Kartashov, L. Zhang, G. G. Paulus, A. Iwasaki, A. Baltuška, K. Yamanouchi, and M. Kitzler, Phys. Rev. X **4**, 021005 (2014).

[16] X. Gong, Q. Song, Q. Ji, H. Pan, J. Ding, J. Wu, and H. Zeng, Phys. Rev. Lett. **112**, 243001 (2014).

[17] A. Méry, A. N. Agnihotri, J. Douady, X. Fléchard, B. Gervais, S. Guillous, W. Iskandar, E. Jacquet, J. Matsumoto, J. Rangama, F. Ropars, C. P. Safvan, H. Shiromaru, D. Zanuttini, and A. Cassimi, Phys. Rev. Lett. **118**, 233402 (2017).

[18] J. Ma, H. Li, K. Lin, Q. Song, Q. Ji, W. Zhang, H. Li, F. Sun, J. Qiang, P. Lu, X. Gong, H. Zeng, and J. Wu, Phys. Rev. A **97**, 063407 (2018).

[19] B. Jochim, R. Erdwien, Y. Malakar, T. Severt, B. Berry, P. Feizollah, J. Rajput, B. Kaderiya, W. L. Pearson, K. D. Carnes, A. Rudenko, and I. Ben-Itzhak, New J. Phys. **19**, 103006 (2017).

[20] S. Larimian, S. Erattupuzha, E. Lötstedt, T. Szidarovszky, R. Maurer, S. Roither, M. Schöffler, D. Kartashov, A. Baltuška, K. Yamanouchi, M. Kitzler, and X. Xie, Phys. Rev. A **93**, 053405 (2016).

[21] M. Alagia, P. Candori, S. Falcinelli, M. S. P. Mundlm, F. Pirani, R. Richter, M. Rosi, S. Stranges, and F. Vecchiocattive, J. Chem. Phys. **135**, 144304 (2011).

[22] M. Alagia, P. Candori, S. Falcinelli, M. Lavollee, F. Pirani, R. Richter, S. Stranges, and F. Vecchiocattive, J. Phys. Chem. A **113**, 14755 (2009).
[23] A. S. Newton and A. F. Sciamanna, J. Chem. Phys. **52**, 327 (1970).
[24] M. Alagia, P. Candori, S. Falcinelli, M. Lavollée, F. Pirani, R. Richter, S. Stranges, and F. Vecchiocattivi, Chem. Phys. Lett. **432**, 398 (2006).
[25] S. Taylor, J. H. D. Eland, and M. Hochlaf, J. Chem. Phys. **124**, 204319 (2006).
[26] M. Kübel, A. S. Alnaser, B. Bergues, T. Pischke, J. Schmidt, Y. Deng, C. Jendrzejewski, J. Ullrich, G. G. Paulus, A. M. Azzeer, U. Kleineberg, R. Moshammer, and M. F. Kling, New J. Phys. **16**, 065017 (2014).
[27] A. Khan and D. Misra, J. Phys. B: At. Mol. Opt. Phys. **49**, 055201 (2016).
[28] P. Bhatt, R. Singh, N. Yadav, and R. Shanker, Phys. Rev. A **86**, 052708 (2012).
[29] N. A. Love and S. D. Price, Phys. Chem. Chem. Phys. **6**, 4558 (2004).
[30] J. H. D. Eland and V. J. Murphy, Rapid Commun. Mass Spectrom. **5**, 221 (1991).
[31] D. M. Curtis and J. H. D. Eland, Int. J. Mass Spectrom. Ion Processes **63**, 241 (1985).
[32] S. D. Price, J. H. D. Eland, P. G. Fournier, J. Fournier, and P. Millie, J. Chem. Phys. **88**, 1511 (1988).
[33] N. Levasseur and P. Millié, J. Chem. Phys. **92**, 2974 (1990).
[34] X. Zhou, P. Ranitovic, C. W. Hogle, J. H. D. Eland, H. C. Kapteyn, and M. M. Murnane, Nat. Phys. **8**, 232 (2012).
[35] A. Hishikawa, A. Iwamae, K. Hoshina, M. Kono, and K. Yamanouchi, Res. Chem. Intermed. **24**, 765 (1998).
[36] M. Ueyama, H. Hasegawa, A. Hishikawa, and K. Yamanouchi, J. Chem. Phys. **123**, 154305 (2005).
[37] L. Chen, X. Shan, X. Zhao, X. L. Zhu, X. Q. Hu, Y. Wu, W. T. Feng, D. L. Guo, R. T. Zhang, Y. Gao, Z. K. Huang, J. G. Wang, X. Ma, and X. J. Chen, Phys. Rev. A **99**, 012710 (2019).
[38] B. Siegmann, U. Werner, H. O. Lutz, and R. Mann, GSI Scientific Report No. 2002 (GSI, Darmstadt, Germany, 2003), p. 100, https://repository.gsi.de/record/53529/files/GSI-Report-2003-1.pdf.
[39] D. Wang, G. Guo, G. Min, and X. Zhang, Phys. Rev. A **95**, 012705 (2017).
[40] X. Ma, X. Zhu, H. Liu, B. Li, S. Zhang, S. Cao, W. Feng, and S. Xu, Sci. China Ser. G: Phys. Mech. Astron. **51**, 755 (2008).
[41] X. Ma, R. T. Zhang, S. F. Zhang, X. L. Zhu, W. T. Feng, D. L. Guo, B. Li, H. P. Liu, C. Y. Li, J. G. Wang, S. C. Yan, P. J. Zhang, and Q. Wang, Phys. Rev. A **83**, 052707 (2011).
[42] W. C. Wiley and I. H. McLaren, Rev. Sci. Instrum. **26**, 1150 (1955).